

## Electrochemical Properties of Nanocomposite Nanoporous Carbon / Nickel Hydroxide

O.M. Hemiy<sup>1</sup>, L.S. Yablon<sup>1,\*</sup>, I.M. Budzulyak<sup>1</sup>, S.I. Budzulyak<sup>2</sup>, O.V. Morushko<sup>1</sup>, A.I. Kachmar<sup>1</sup>

<sup>1</sup> *Vasyl Stefanyk Precarpathian National University, 57, Shevchenko st., 76018 Ivano-Frankivsk, Ukraine*

<sup>2</sup> *V.E. Lashkaryov Institute of Semiconductor Physics NAS of Ukraine, 41, Nauki pr., 03028 Kyiv-28, Ukraine*

(Received 30 August 2016; published online 23 December 2016)

The electrochemical properties of composite nanoporous carbon / nickel hydroxide as electrode material for hybrid supercapacitors were investigated. Fast reversible faradaic reactions flow was determined in connection with chemical makeup of the  $\beta$ -Ni(OH)<sub>2</sub>/C composite. It is shown that increase of nickel hydroxide concentration can intensify reactions. It is found that clean  $\beta$ -Ni(OH)<sub>2</sub> has 238 F/g of specific capacity, but  $\beta$ -Ni(OH)<sub>2</sub>/C nanocomposite with 90 % nickel hydroxide has 292 F/g. Such capacity value can be considered as a maximum for these composites.

**Keywords:** Composite, Nickel hydroxide, Nanoporous carbon, Specific capacity

DOI: [10.21272/jnep.8\(4\(2\)\).04074](https://doi.org/10.21272/jnep.8(4(2)).04074)

PACS numbers: 81.05.Rm, 81.05.Uw, 81.16. ± c, 81.40.Wx

### 1. INTRODUCTION

For now, activated carbon based supercapacitors (SC) with double electric layer (DEL) have specific capacity parameters that still do not match the requirements of modern electronics and engineering. Improvement rate of carbon electrode materials has already reached some certain limit – SC parameters average increase hardly exceeds 1-2 %. In order to push this limit higher we need to use pseudocapacity and processes that take place in the hybrid electrochemical systems. In addition to the classic electrical charge storage on the DEL, capacity of pseudo- or oxidation-reduction capacitors highly depends on the fast reversible faradaic electrochemical processes. This approach allows to get more than 10x increase of differential capacity in comparison with activated carbon based SCs that have DEL as the main charge storage.

Hydroxides/oxides of metals and some polymers were investigated to form SC with increased specific capacity and high energy density. It is identified that the best electrode materials for SC [1] can be based on the noble metals oxides (ruthenium oxide, for example) that provide faradaic pseudocapacity. However, ruthenium oxide (even with its high specific capacity) is too expensive for the commercial use. Therefore, researchers' attention is concentrated on the alternative electrode materials search. They should be cheap enough and show capacitance behaviour analogical to the ruthenium oxide. In particular, good alternative is nickel hydroxide.

It is known [2] that nickel hydroxide has three polymorphs:  $\alpha$ -,  $\beta$ - and  $\gamma$ -Ni(OH)<sub>2</sub>.  $\alpha$ -phase has higher theoretical capacity, but is unstable in an alkaline environment and quickly turns into  $\beta$ -Ni(OH)<sub>2</sub>, that is more stable [3].  $\gamma$ -Ni(OH)<sub>2</sub> does not have reversibility, that's why it can't be used as a capacitor electrode material. To intensify electrochemical processes in systems formed using nickel hydroxide, authors [4-6] have used heteroatoms of Co and Zn doping. For example, Co behaves like an important catalyst for the electron-

based conductivity rate, and Zn can make the crystalline grates structure of Ni(OH)<sub>2</sub> looser to heighten ions dynamic [6]. To increase specific surface area, authors [4] have prepared nanostructural (or porous) Ni(OH)<sub>2</sub>. In [7] Ni(OH)<sub>2</sub>/graphene and RuO<sub>2</sub>/graphene were used as electrode materials of an asymmetric SC. The specific capacitance of such device was 153 F/g.

Thus, nickel hydroxide and nanoporous carbon usage in nanocomposite electrodes looks promising. They will provide rapid reversible faradaic processes in corresponding electrolytes and can be good choice for SC with pseudocapacity.

### 2. OBJECTS AND METHODS

Six groups of composites, in which the content of nanoporous carbon produced from the vegetable raw by its hydrothermal carbonization and activation [8] amounted to 10, 20, 30, 50, 70, and 90 mass %, were prepared using mechanochemical method. The resulting composites were mixed with a conductive additive (acetylene soot) in the 75:25 % proportions and deposited on nickel mesh 0.49 cm<sup>2</sup> in size to form electrodes.

In order to study the electrochemical behavior of composite materials in aqueous electrolytes we used three-electrode electrochemical cells. The materials under study served as the working electrodes, a platinum electrode as an auxiliary, and Ag/AgCl electrode as a reference one. The 33 % KOH aqueous solution was used as the electrolyte. The influence of composition of electrode material on the electrochemical properties and cyclic properties of energy storage devices were studied using impedance spectroscopy, cyclic voltammetry, and charge-discharge testing. The electrochemical studies were carried out by galvanostatic and potential dynamic methods using an Autolab PGSTAT/FRA-2 spectrometer.

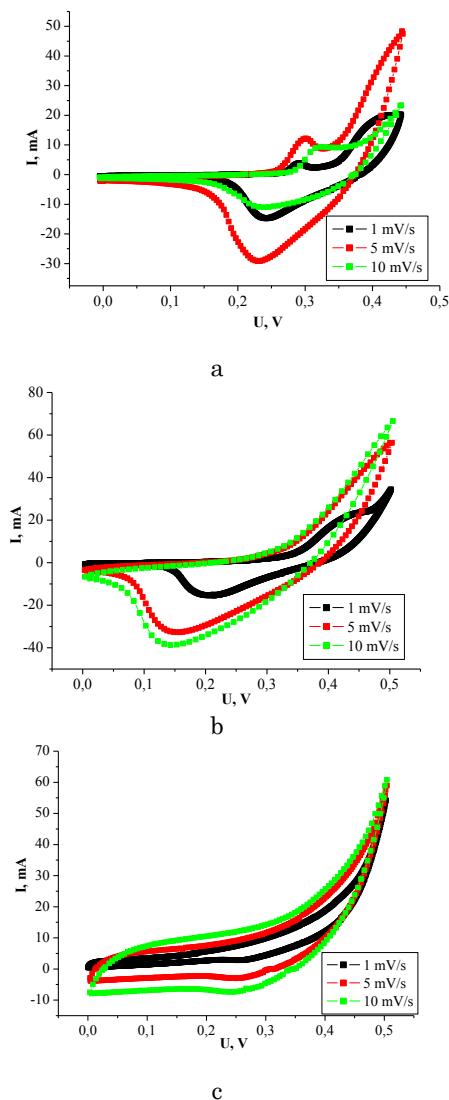
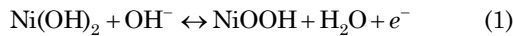
### 3. DISCUSSION OF RESULTS

Figure 1 shows the cyclic voltamperograms (CVA)

\* [yablon\\_lyubov@ukr.net](mailto:yablon_lyubov@ukr.net)

for the pure  $\beta$ -Ni(OH)<sub>2</sub> (a) and its composites with different carbon content (b, c) at the voltage scan rates of 1, 5, and 10 mV/s. A characteristic feature of the electrochemical system behavior is that two redox peaks responsible for the pseudocapacity are observed in the voltamperogram of pure  $\beta$ -Ni(OH)<sub>2</sub> (Fig. 1, a). One of them at 0.29 V (voltage scan rate is 5 mV/s) is the anode peak (positive current density) caused by oxidation of Ni(OH)<sub>2</sub> to NiOOH. This peak corresponds to the charging process. Another peak at 0.24 V is the cathode one (negative current density) and corresponds to the discharging process.

These peaks correspond to fast reversible redox processes at the Ni(OH)<sub>2</sub>/electrolyte interface which are described by the following chemical equation:



**Fig. 1** – Cyclic voltammograms of pure  $\beta$ -Ni(OH)<sub>2</sub> (a) and  $\beta$ -Ni(OH)<sub>2</sub>/C composites with the composition relationship  $\beta$ -Ni(OH)<sub>2</sub>:C = 90:10 (b), 10:90 (c)

With an increase in carbon content, anode peak shifts towards higher voltages, while cathode peak towards lower ones (Fig. 1 b, c). With that, the height of peaks in CVA curves decreases with the carbon content

increase, and at a carbon content of 90 mass % of the electrode (Fig. 1 c) peaks are almost not observed.

As shown in [9], separate K<sup>+</sup> cations may also participate in redox reactions on the Ni(OH)<sub>2</sub> surface. This indicates that the capacitance characteristics are governed not only by the DEL capacity, but the Faraday reactions too. Moreover, the shape of CVA curves indicates that the capacitive characteristic of these materials differs from that of DEL; the shape of CVA curve is usually close to a perfect rectangular one, which may mean that the nickel hydroxide redox reactions are diffusion limited ones. In addition, the electrodes based on the composites with carbon as conductive material have more integrated areas at different voltage scan rates, i.e., the powder of active Ni(OH)<sub>2</sub> material can reach a relatively higher capacity. An increase in the carbon mass content may contribute to the formation of larger particles or large agglomerates, which leads to the deterioration of the electrical conductivity due to inhibition of ion diffusion on the electrode.

Specific capacity of the nanocomposite electrodes has been evaluated from the CVA curves by integrating the area under the cathode current curve  $I(U)$  in an interval from anode limiting voltage  $U_a$  to cathode limiting voltage  $U_k$  and dividing result by the voltage scan rate  $S$ , nanocomposite mass, and voltage window  $U_a - U_k$  according to the following formula:

$$C = \frac{A}{(U_a - U_k)mS} \quad (2)$$

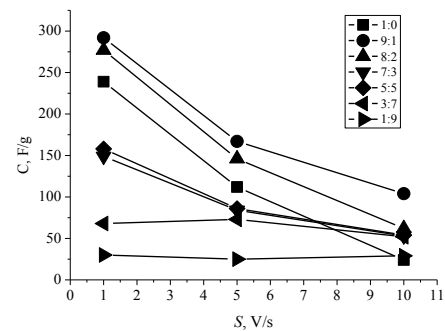


**Fig. 2** – Specific capacity as function of voltage scan rate for pure  $\beta$ -Ni(OH)<sub>2</sub> and  $\beta$ -Ni(OH)<sub>2</sub>/C composites with the composition relationship  $\beta$ -Ni(OH)<sub>2</sub>:C = 90:10, 80:20, 70:30, 50:50, 30:70, and 10:90

As seen from Fig. 2, at a voltage scan rate of 1 mV/s specific capacity of the pure  $\beta$ -Ni(OH)<sub>2</sub> and nanocomposite with  $\beta$ -Ni(OH)<sub>2</sub>:C = 90:10 amounts to 238 and 292 F/g, respectively, while at a voltage scan rate of 10 mV/s this value reduces to 24 F/g for the pure  $\beta$ -Ni(OH)<sub>2</sub> and to 104 F/g for the composite. This may be caused by an efficient transport of ions in the pores of the active materials at low voltage scan rate, while at a higher voltage scan rate some active surface areas become inaccessible for charge accumulation.

An increase in the carbon content and, accordingly, decrease of the nickel hydroxide mass in the nanocomposite affect the specific capacity value stronger than the increase in the carbon surface area. This serves as convincing evidence that specific capacity of  $\beta$ -Ni(OH)<sub>2</sub>/C nanocomposite is regulated by  $\beta$ -Ni(OH)<sub>2</sub>

redox reactions. Due to the increased surface area, carbon provides more active centers for the Faraday reactions and results in the electrode resistivity decrease. Thus, it was found that the optimum amount of carbon is about 10 % of the composite mass.

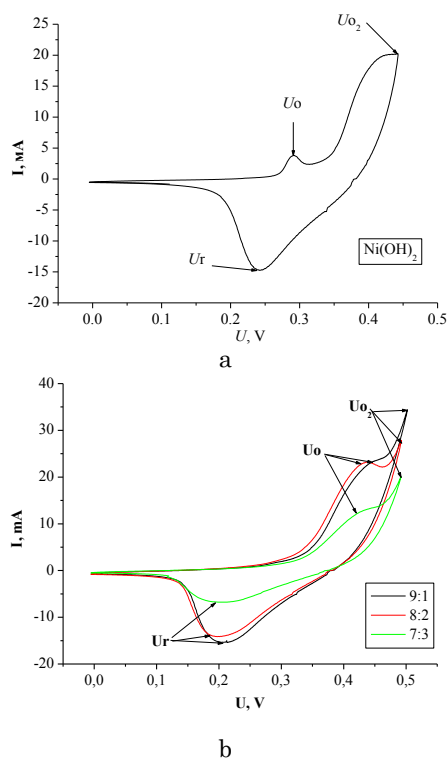


**Fig. 3** – CVA of pure  $\beta\text{-Ni(OH)}_2$  (a) and composites (b) at a voltage scan rate of 1 mV/s

As seen from the Fig. 3a the oxidation peak for the pure  $\beta\text{-Ni(OH)}_2$  corresponds to  $U_o = 0.29$  V, while the cathode recovery peak is observed at  $U_r = 0.24$  V resulting in the potential difference  $U_o - U_r = 0.05$  V. When carbon is added, the anode peak shifts towards larger potential values, while cathode peak position almost does not change.

In particular,  $U_o = 0.44$  V for the  $\beta\text{-Ni(OH)}_2$ -based composites with a carbon content of 10, 20, 30 % (Figs. 3b), while for composites with a maximum carbon content the oxidation peak practically vanishes and can not be fixed. This indicates that the redox reactions are inhibited, and the charge accumulates only due to the DEL formation on the carbon material. A shift of the anode peak of current is usually associated with the impurities, NiOOH nucleation, and increase in the concentration of nickel ions ( $\text{Ni}^{2+}$  or  $\text{Ni}^{3+}$ ). Increase of the oxidation current peak and decrease of the recovery current peak are the results of the excellent electrocatalytic activity of  $\beta\text{-Ni(OH)}_2/\text{C}$  nanocomposites.

Detailed features of the CVAs are presented in Table 1. The potential difference  $U_o - U_r$  between the anode and cathode peak positions is associated with the reversibility of the electrode reaction.

Galvanostatic charge-discharge measurements were performed at the currents of 5 and 10 mA in a potential window of 0-0.4 V. The asymmetry of the charge-discharge curves (Fig. 4) is the consequence of the irre-

versible kinetic changes occurring in the electrolyte and electrode materials due to redox reactions.

**Table 1** – Redox CVA peaks for the pure  $\beta\text{-Ni(OH)}_2$  and its composites with different carbon content.

Electrode	Potential, V					Current, mA	
	$U_r$	$U_o$	$U_{o2}$	$U_o - U_r$	$U_{o2} - U_o$	Recovery peak	Oxidation peak
$\beta\text{-Ni(OH)}_2$	0.24	0.29	0.45	0.05	0.16	-14.7	3.8
90:10	0.21	0.44	0.5	0.23	0.06	-15.3	22.9
80:20	0.2	0.44	0.5	0.22	0.06	-14	23.2
70:30	0.21	0.44	0.5	0.23	0.06	-6.8	13
50:50	0.20	0.44	0.5	0.24	0.06	-9.4	19.5
30:70	0.25	–	0.5	–	–	-4.6	21.5
10:90	–	–	0.5	–	–	–	–

\*  $U_r$  is the recovery peak potential,  $U_o$  is the oxidation peak potential, and  $U_{o2}$  is the potential of oxygen release.

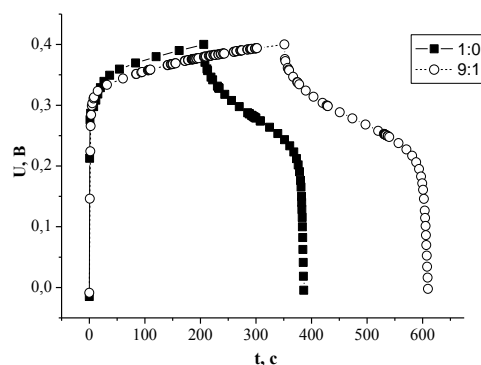


**Fig. 4** – Charge-discharge curves of the pure  $\beta\text{-Ni(OH)}_2$  and  $\beta\text{-Ni(OH)}_2/\text{C}$  nanocomposite with the composition relationship 90:10

As Fig. 5 shows, discharge curves are nonlinear. In a range of 0.4-0.2 V their nonlinearity is associated with the pseudocapacity of the materials, while in a range of 0.2-0 V linear regions are related to the capacity of DEL formed on the electrode/electrolyte interface. A potential plateau on the discharge curves (Fig. 5) is observed both for pure  $\beta\text{-Ni(OH)}_2$  and composites indicating that the process of nickel recovery is the dominant one. However, with an increase in the current value and carbon content, the discharge potential plateau is reduced and almost disappears when the carbon content exceeds 70 %.

The specific capacity value (Fig. 6) calculated from the discharge curves at a current of 5 mA amounts to 220 F/g for the  $\beta\text{-Ni(OH)}_2/\text{C}$  composite with composition relationship 90:10 and 176 F/g for the composite with composition relationship 80:20 and is larger than 156 F/g for pure  $\beta\text{-Ni(OH)}_2$ , which is well consistent with data obtained from the CVA curves and those presented in [10].

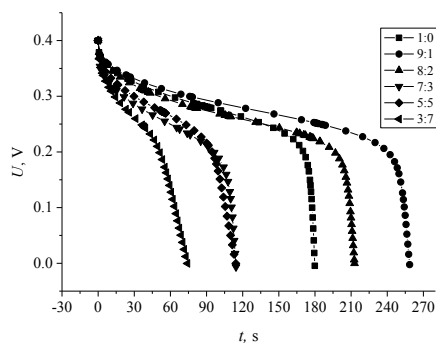


**Fig. 5** – Discharge curves of the composites with different carbon content at a current of 5 mA

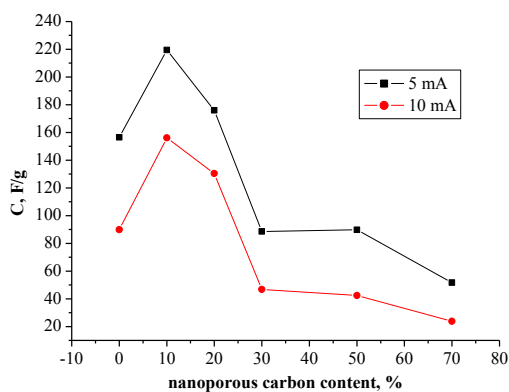


**Fig. 6** – Specific capacity calculated from the galvanostatic discharge curves for the electrodes with different carbon content at the currents of 5 and 10 mA

A high specific capacity of the electrode materials with low electronic resistance can be achieved; for this reason they are effective when used in electrochemical energy storage devices. Electrochemical impedance spectroscopy is a method used to evaluate the resistance of the electrode material and electrolyte solution. Nyquist diagrams for pure  $\beta\text{-Ni(OH)}_2$  and composites with different carbon content which were taken at an initial potential of the cells in a frequency range from 0.01 Hz to 105 Hz are shown in Fig. 7. At high frequencies a small region in the form of semicircle is observed, which indicates the presence of a resistance to charge transfer caused by the Faraday processes at the electrode/electrolyte interface, due to which a solid-state film transparent for potassium ions is formed on the composite surface. The straight Warburg line in the low frequency range, which is inclined to the real axis at an angle of about  $60^\circ$ , corresponds to the mass transfer. On the basis of Nyquist diagrams and using ZView2 program, we have modeled an equivalent circuit diagram (ECD) (Fig. 8), which consists of series-connected electrolyte resistance  $R_0$ ,  $R_1$ -CPE1 link (where CPE means constant phase element) modeling DEL formation at the particle/electrolyte interface,

$R_2$ -CPE2 link modeling the process of redox reactions, and CPE3 element for which  $\text{K}^+$  ion diffusion is responsible.

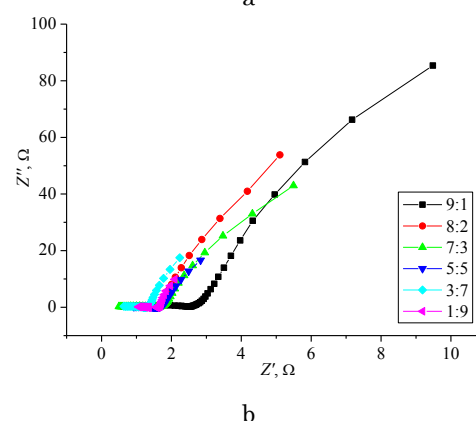
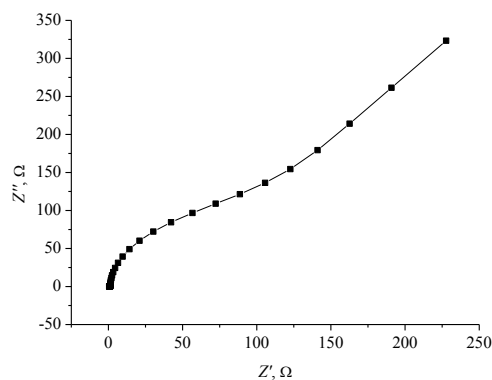


**Fig. 7** – Nyquist diagrams for pure  $\beta\text{-Ni(OH)}_2$  (a) and composites with different carbon content (b)

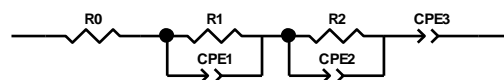


**Fig. 8** – ECD of pure  $\beta\text{-Ni(OH)}_2$  and composites with different carbon content.

#### 4. CONCLUSIONS

1. The character of fast reversible Faraday reactions as function of the  $\beta\text{-Ni(OH)}_2/\text{C}$  composition content is determined. It is found that with an increase in the nickel hydroxide content the intensity of these reactions increases. In particular, at 90 % nickel hydroxide content in the composite the oxidation and recovery peaks, which are observed in the vicinity of 0.29 V and 0.24 V, respectively, reach their maximum values.

2. It is found that pure  $\beta\text{-Ni(OH)}_2$  has specific capacity of 238 F/g, whereas  $\beta\text{-Ni(OH)}_2/\text{C}$  nanocomposite with 90 % nickel hydroxide content has 292 F/g specific capacity, which is the maximum one for the composites studied in this work.

## REFERENCES

1. Q. Huang, X. Wang, J. Li, C. Dai, A. Gambia, P.J. Sebastian, *J. Power Sources* **164**, 425 (2007).
2. P. Oliva, J. Leonardi, J.F. Laurent, C. Delmas, J.J. Bracco, M. Figlarz, F. Fievet, A. de Guibert, *J. Power Sources* **8**, 229 (1982).
3. J. W. Lang, L. B. Kong, M. Liu, Y. C. Luo, L. Kang, *J. Solid State Electr.* **14**, 1533 (2010).
4. J.H. Zhong, A.L. Wang, G.R. Li, J.W. Wang, Y.N. Ou, Y.X. Tong, *J. Mater. Chem.* **22**, 5656 (2010).
5. G.P. Wang, L. Zhang, J. Kim, J.J. Zhang, *J. Power Sources* **217**, 554 (2012).
6. J.H. Park, S.W. Kim, O. Park, J.M. Ko, *Appl. Phys. A: Mater. Sci. Process.* **82**, 593 (2006).
7. H. Wang, Y. Liang, T. Mirfakhrai, Z. Chen, H.S. Casalongue, H. Dai, *Nano Research* **4**, 729 (2011).
8. B.K. Ostafiychuk, I.M. Budzulyak, I.F. Myronyuk, I.I. Grygorchak, *Nanomaterialy v prystroyah generuvannya i nakopychennya energii* (Ivano-Frankivsk: 2007) [in Ukrainian].
9. Chi-Chang Hu, Kuo-Hsin Chang, Tung-Yu Hsu, *J. Electrochem. Soc.* **155**, F196 (2008).
10. O. Khemiy, I. Budzulyak, L. Yablon, D. Popovych, O. Morushko, *Nanosystems, Nanomaterials, Nanotechnologies* **14**, 147 (2016).